



# Degradation of sulfonated polyethylene by a bio-photo-fenton approach using glucose oxidase immobilized on titanium dioxide

Sunil Ghatge<sup>a,1</sup>, Youri Yang<sup>a,1</sup>, Yongseok Ko<sup>a</sup>, Younggun Yoon<sup>b</sup>, Jae-Hyung Ahn<sup>b</sup>, Jeong Jun Kim<sup>b,\*</sup>, Hor-Gil Hur<sup>a,\*</sup>

<sup>a</sup> School of Earth Sciences and Environmental Engineering, Gwangju Institute of Science and Technology (GIST), Gwangju 61005, Republic of Korea

<sup>b</sup> Bioremediation Team, National Institute of Agricultural Science, 166 Nongsaeangmyeong-ro, Iseo-myeon, Wanju-gun, Jeollabuk-do 55365, Republic of Korea

## ARTICLE INFO

Editor: Dr. R Teresa

### Keywords:

Biocatalysis  
Bio-Fenton  
Hydrogen peroxide  
Hydroxyl radicals  
Photo-catalysis

## ABSTRACT

Polyethylene (PE) plastics are highly recalcitrant and resistant to photo-oxidative degradation due to its chemically inert backbone structure. We applied two novel reactions such as, Bio-Fenton reaction using glucose oxidase (GOx) enzyme alone and Bio-Photo-Fenton reaction using GOx immobilized on TiO<sub>2</sub> nanoparticles (TiO<sub>2</sub>-GOx) under UV radiation, for (bio)degradation of pre-activated PE with sulfonation (SPE). From both the reactions, GC-MS analyses identified small organic acids such as, acetic acid and butanoic acid as a major metabolites released from SPE. In the presence of UV radiation, 21 fold and 17 fold higher amounts of acetic acid (4.78 mM) and butanoic acid (0.17 mM) were released from SPE after 6 h of reaction using TiO<sub>2</sub>-GOx than free GOx, which released 0.22 mM and 0.01 mM of acetic acid and butanoic acid, respectively. Our results suggest that (bio)degradation and valorization of naturally weathered and oxidized PE using combined reactions of biochemistry, photochemistry and Fenton chemistry could be possible.

## 1. Introduction

Fossil fuel based synthetic polymers such as polyethylene (PE), polystyrene (PS), polypropylene (PP), polyvinyl chloride (PVC), polyurethane (PUR), polyethylene terephthalate (PET), called plastics, have become indispensable parts of every aspect of our lives. With growing demand of the plastics around the world, it has been predicted that more than 26 billion tons of plastic wastes will be produced by 2050 (Jambeck et al., 2015; Lönnstedt and Eklöv, 2016; Geyer et al., 2017). As high as 79% of the plastic wastes is discarded into landfill or scattered into natural environments including the oceans, causing serious environmental issues in the various ecosystems (North and Halden, 2013). Along with landfilling, the plastic wastes were treated either via incineration or by catalytic pyrolysis methods. These methods are associated with problems like lack of empty places for landfilling, generation of secondary pollutants such as carbon monoxide (CO) and nitrogen oxides (NOx) during incineration, use of high temperature typically >400 °C in the pyrolysis, and expensive catalysts in heterogeneous catalytic reactions (Aguado et al., 2008; Serrano et al., 2012; Rahimi and García, 2017). Therefore, it is of prime requirement to develop an innovative

and promising approaches for the degradation and recycling of the plastic wastes. PE and PP plastics contribute immensely to the total plastic production with the amounts of over 100 million metric tons (Mehmet, 2011). Unlike PET and PU, PE and PP plastics do not contain hydrolysable functional groups in the C-C and C-H structures, which make them difficult to (bio)degrade without pretreatments hence, they are persistent in the environment for years. In addition, the physicochemical properties of PE such as hydrophobicity, degree of crystallinity, surface topography and molecular size also play an important role in its recalcitrance (Tokiwa et al., 2009; Restrepo-Florez et al., 2014). Therefore, the oxidation of stable C-C and C-H bonds in the PE plastics with forming oxidized functional groups such as carboxyl, carbonyl, ether, and hydroxyl is the prime requirement for its further depolymerization (Zheng et al., 2005; Restrepo-Florez et al., 2014). Thus, various physicochemical pretreatments such as UV irradiation (Albertsson et al., 1987; Albertsson and Karlsson, 1990), chemical oxidizing agents (Brown et al., 1974), thermo-oxidation (Lee et al., 1991), etc. have been applied to produce the reactive oxygen species (ROS) such as hydroxyl radicals (•OH), superoxide radical anions (O<sub>2</sub>•<sup>-</sup>), and hydroperoxyl radicals (•OOH), which could be involved in the

\* Corresponding authors.

E-mail addresses: [jjkim66@korea.kr](mailto:jjkim66@korea.kr) (J.J. Kim), [hghur@gist.ac.kr](mailto:hghur@gist.ac.kr) (H.-G. Hur).

<sup>1</sup> Sunil Ghatge and Youri Yang are contributed equally to this work.

formation of the oxidized functional groups. Among ROS, the  $\bullet\text{OH}$  radical has the strongest oxidation capacity with oxidation potential ( $E_0$ ) of 2.73 V (Babuponnusami and Muthukumar, 2014; Nidheesh, 2015). The conventional Fenton reaction produces the  $\bullet\text{OH}$  radical from  $\text{H}_2\text{O}_2$  in the presence of ferrous ions as a catalyst (Babuponnusami and Muthukumar, 2014; Nidheesh, 2015). Due to its simplicity, high efficiency, and versatility, the Fenton processes are commonly employed in wastewater treatments for the degradation and mineralization of various hazardous organic pollutants (Pignatelli et al., 2006; Babuponnusami and Muthukumar, 2014; Nidheesh, 2015). The Fenton reaction is capable of either complete mineralization of pollutants to  $\text{CO}_2$ ,  $\text{H}_2\text{O}$ , and inorganic salts, or partially degrades them to low-molecular-weight fragments, depending on the reaction conditions such as types of Fenton reagents and solvents, pH, reaction time, or use of irradiation (Kavitha and Palanivelu, 2004; Deng and Englehardt, 2006).

Apart from the conventional Fenton reaction, the  $\bullet\text{OH}$  radicals can be generated using various non-conventional methods or the combination of both such as Fenton-like, Photo-Fenton, Sono-Fenton, Electro-Fenton, Sono-Electro-Fenton, Photo-Electro-Fenton, Sono-Photo-Fenton, etc (Babuponnusami and Muthukumar, 2014; Nidheesh, 2015). The conventional Fenton reaction efficiency was affected by the regeneration rate of  $\text{Fe}^{3+}$  to  $\text{Fe}^{2+}$ . This in-situ circulation from  $\text{Fe}^{3+}$  to  $\text{Fe}^{2+}$  can be achieved with a combination of  $\text{H}_2\text{O}_2$  and UV radiation with  $\text{Fe}^{2+}$  or  $\text{Fe}^{3+}$  ions. The process is known as a Photo-Fenton reaction, which involves photochemical regeneration of  $\text{Fe}^{2+}$  by photo-reduction of  $\text{Fe}^{3+}$ . Additionally, direct photolysis of  $\text{H}_2\text{O}_2$  also occurs in presence of UV radiation, resulting into enhanced production of  $\bullet\text{OH}$  radicals and increased degradation of organic pollutants compared to the conventional Fenton method (Zepp et al., 1992; Zuo and Hoigné, 1992).

It has been known that biochemical reactions also can activate oxygen molecules to incorporate them into various organic molecules, including alkanes, arenes, and lignin (Burek et al., 2019; Chan et al., 2020). Thus, microbes and their degradative enzymes have been tested for biodegradation of PE plastics. Lignin degrading enzymes including laccases (EC 1.10.3.2), manganese peroxidase (MnP, EC 1.11.1.13) and lignin peroxidases (LiP, EC 1.11.1.14) have been reported to be involved in the biodegradation of PE (Santo et al., 2013; Restrepo-Florez et al., 2014; Krueger et al., 2015). Alkane hydroxylases (AH) (EC 1.14.15.3) catalyzing the degradation of hydrocarbon oligomers by terminal or subterminal oxidation have been reported to convert 20% of the LDPE sample to  $\text{CO}_2$  after incubation for 80 days at 37 °C (Yoon et al., 2012). Additionally, recombinant *E. coli* cells expressing the complete AH system from *Pseudomonas aeruginosa* E7 degraded about 30% of the PE sample (Jeon and Kim, 2015). However, most of the PE biodegradation studies analyzed changes of the various physicochemical properties of PE such as weight loss, structural changes, and modifications of functional groups, etc (Restrepo-Florez et al., 2014; Sen and Raut, 2015). Recently, it has been criticized that the above mentioned changes in the physicochemical properties can be associated with the degradation of various additives, which often contribute to significant fraction of the PE (Weber et al., 2017; Danso et al., 2019; Ghatge et al., 2020). Also, none of these studies reported the identification and quantification of candidate metabolites produced from PE (Yoon et al., 2012; Santo et al., 2013; Jeon and Kim, 2015) which could be a direct evidence for real PE biodegradation.

Recently, microbes or enzyme supported Fenton reactions were immersed as a sustainable alternative method for degrading organic pollutants (Karimi et al., 2012; Gu et al., 2016; Wang et al., 2020). It is a promising method with low power consumption along with the ability of in-situ generation of  $\text{H}_2\text{O}_2$ , which reduces chances of accidents during the transportation, storage of  $\text{H}_2\text{O}_2$  and overall financial expenses (Kahousha et al., 2018). In addition, many bacterial species associated with the human body including *Streptococcus pyogenes*, *Streptococcus pneumoniae*, *Streptococcus oralis*, *Bifidobacterium bifidum*, *Lactobacillus johnsonii*, *Lactobacillus crispatus*, and *Lactobacillus jensenii*, were capable

of producing  $\text{H}_2\text{O}_2$  (Hertzberger et al., 2014). In the central carbon and energy metabolism,  $\text{H}_2\text{O}_2$  is mainly produced by various oxidases such as lactate oxidase (LOx), pyruvate oxidase (POx), NADH oxidases (Nox), oxalate oxidase (OXO), glucose oxidase (GOx), etc (Condon, 1987; Bankar et al., 2009; Hu et al., 2015). These oxidases could be potential candidates for in-situ  $\text{H}_2\text{O}_2$  production in the Bio-Fenton reaction.

Among the above oxidases, glucose oxidase (GOx) is the most commonly used enzyme in the Bio-Fenton reaction, which catalyzes the oxidation of D-glucose to form D-glucono-1,5-lactone with the formation of  $\text{H}_2\text{O}_2$  and superoxide as a by-product in presence of dioxygen (Su and Klinman, 1999; Bankar et al., 2009). This enzymatic reaction is already used in various industries such as biosensor development, food processing, wineries, oral hygiene products, gluconic acid production, and bleaching in the textile industry (Bankar et al., 2009). Until now, the GOx dependent Fenton reaction is predominantly applied for degradation of various textile dyes and trichloroethylene (Karimi et al., 2012; Eskandarian et al., 2013; Ravi et al., 2020). In addition, UV assisted efficient degradation of malachite green and methylene blue using GOx immobilized on titanium dioxide ( $\text{TiO}_2$ ) nanoparticles as a bio-organic-inorganic hybrid photocatalyst have been investigated (Kim et al., 2019; Dong et al., 2020).

Chow et al. (2016) introduced combination of chemical activation and use of Photo-Fenton reactions for valorization of waste PE. PE was pre-activated with sulfonation ( $-\text{SO}_3$ ) by chlorosulfuric acid under refluxing conditions, followed by grafting of  $\text{Fe}^{3+}$  catalysts onto the surface of the polymer chains thereby forming sulfonated and iron-grafted PE (SPE). Further treatments with hydrogen peroxide, which leads to the Fenton reactions, can degrade SPE into various carboxylic acids (Chow et al., 2016, 2018).

In this study, we tested the Bio-Fenton and Bio-Photo-Fenton reactions in an attempt to degrade SPE using free GOx and GOx enzyme immobilized on  $\text{TiO}_2$  nanoparticles ( $\text{TiO}_2$ -GOx) for in-situ generation of  $\text{H}_2\text{O}_2$ . We identified small organic acids including acetic acid and butanoic acid as major products released from SPE using both the Bio-Fenton reactions. In the Bio-Photo-Fenton reaction, when UV light was exposed to the reaction system, containing  $\text{TiO}_2$ -GOx, the amounts of products were increased significantly. Considering various biochemical reactions that support  $\text{H}_2\text{O}_2$  production, the current results suggest that biochemically-, and photochemically-assisted Fenton reactions could be applied for degrading naturally weathered and oxidized polyethylene plastics.

## 2. Materials and methods

### 2.1. Chemicals

PE (average Mw: ~4000; average Mn: ~1700),  $\text{TiO}_2$  nanoparticles (P-25), lyophilized powder of GOx from *Aspergillus niger* (167 U/mg), glutaraldehyde solution (GA, 25%), (3-aminopropyl)triethoxysilane (APTES, 98%), D-(+)-glucose, and ferric chloride were purchased from Sigma Aldrich (St. Louis, MO, USA). Chlorosulfuric acid (98%) was obtained from Kanto chemical co. (Tokyo, Japan). Chloroform and dichloromethane was purchased from Fisher Scientific (Hampton, NH, USA). Hydrochloric acid and 30 wt% hydrogen peroxide was obtained from Duksan pure chemicals Co. Ltd (Ansan, South Korea). The BCA protein assay kit and Amplex® red hydrogen peroxide/peroxidase assay kit were purchased from Invitrogen (Carlsbad, CA, USA). All authentic standard chemicals used in this study were obtained from Sigma-Aldrich with their highest purity grade.

### 2.2. Preparation of pre-activated PE with sulfonation (SPE)

PE powder was treated as reported by Chow et al. for the preparation of SPE (Chow et al., 2016, 2018). Briefly, 2.0 g of PE powder was suspended in 50 mL of refluxing chloroform with stirring (200 rpm). A 15 mL mixture of dichloromethane and chlorosulfuric acid (2:1 v/v) was

added to the suspension over 30 min in a dropwise manner. The brown suspension thus formed was further heated at 65 °C with stirring (200 rpm) for an additional 2 h. The organic solvent was evaporated from the reaction mixture under vacuum followed by addition of FeCl<sub>3</sub> solution (0.75 M, 100 mL) and the mixture was allowed to stir overnight under ambient conditions. The resulting black solid was collected using centrifugation and washed with deionized water until the supernatant became colorless. The solids were oven-dried at 80 °C and stored in an amber colored screw cap reagent bottle until further use.

### 2.3. Bio-Fenton degradation of SPE

In a 50 mL of conical flask, 32 mM of glucose was incubated with 10 U of GOx in 10 mL of 50 mM of phosphate buffer (pH 5.5) containing 10 mg of SPE. The reaction mixtures were incubated at 30 °C with gentle stirring at 100 rpm for 6, 12, 24, and 48 h. Samples were withdrawn periodically to measure the change in pH. Separate control reactions containing GOx enzyme in the absence of SPE, and no GOx enzyme in the presence of SPE were run simultaneously. Ferric citrate in a final concentration of 0.5 mM was added in the reaction mixture where SPE was not present, in order to analyze effect of Fenton reaction on glucose and GOx. For the accurate measurement of in-situ production of H<sub>2</sub>O<sub>2</sub> by GOx during the course of reaction, a separate reaction was carried out simultaneously without SPE and ferric citrate. Furthermore, the effect of different concentration of GOx (2.5 and 10 U) on SPE degradation was analyzed by identifying and measuring metabolites released from SPE after 48 h of reaction. SPE and precipitated materials were separated from the reaction mixture via centrifugation and filtration through 0.2 µm syringe filter. The clarified supernatants were analyzed using GC-MS for identification and quantification of metabolites released from SPE after Bio-Fenton degradation.

### 2.4. Immobilization of glucose oxidase on TiO<sub>2</sub> nanoparticles

TiO<sub>2</sub> nanoparticles (500 mg) surfaces were activated overnight in 50 mL of piranha solution which is a mixture of 1 part of 30% H<sub>2</sub>O<sub>2</sub> and 4 parts of concentrated sulfuric acid, with gentle stirring at room temperature. The activated TiO<sub>2</sub> nanoparticles were further washed several times with sterile distilled water (Baranowski et al., 2016). The activated TiO<sub>2</sub> nanoparticles (250 mg) were functionalized with APTES by suspending them in 10 mL of the APTES aqueous solution (10% v/v). The solution was prepared by mixing 10 mL of the acidified water (pH 4.0) with 1 mL of APTES, followed by 20 min stirring at room temperature. Additionally, 4 mL of glycerol was added and the reaction mixture was incubated at 90 °C for 5 h with constant stirring at 200 rpm (Jaquish et al., 2018). Then, the resulting support was washed three times with sterile deionized distilled water (SDDW) and five times with methanol followed by drying in a vacuum oven overnight. The dried TiO<sub>2</sub>-APTES nanoparticles (0.10 g) was added to 20 mL of glutaraldehyde (GA) solution in the PBS buffer and stirred for 1 h. The GA solution was prepared by adding 0.08 mL of 25% GA solution to 20 mL of the PBS buffer at pH 7.0. The support functionalized with GA was separated using centrifugation and washed five times with PBS and SDDW. Finally, 10 mg of GOx lyophilized powder was added to 20 mL of the PBS containing 100 mg of TiO<sub>2</sub>-APTES-GA functionalized support and stirred for 2 h at RT and overnight at 4 °C. Then, the TiO<sub>2</sub>-APTES-GA-GOx nanoparticles were washed with PBS to remove unbound GOx. TiO<sub>2</sub>-GOx were separated using centrifugation and resuspended in PBS to obtain a 5 mg/mL of particle solution, which was stored at 4 °C until further application. The amount of immobilized GOx on TiO<sub>2</sub> nanoparticles was evaluated by subtracting unbound GOx amount from the initial total GOx amount added at the beginning of the experiment, measured using a BCA protein assay kit (Huang et al., 2011; Kim et al., 2019).

### 2.5. Bio-Photo-Fenton reaction for SPE degradation

The Bio-Photo-Fenton reaction mixtures were prepared as above by replacing free GOx with 10 U of TiO<sub>2</sub>-GOx. The one sun output of entire UV spectra was obtained using low cost solar simulator from ABET Technologies (Milford, CT, USA) fitted with ozone-free Xe Arc Lamp (150 W). 400 nm cut-off filter was used and the distance between the light source and the sample surface was adjusted to 10 cm. The samples were exposed to solar UV spectra for 2, 4, and 6 h at 30 °C in water bath with stirring at 160 rpm. The samples were centrifuged at 5000 rpm for 5 min to remove the SPE and TiO<sub>2</sub>-GOx. The supernatant was analyzed for products released from SPE as described above. The control experiments containing free GOx and the TiO<sub>2</sub> nanoparticles alone in the presence of SPE were performed simultaneously.

### 2.6. GC-MS analysis for identification and quantification of metabolites released from SPE

The filtered (0.2 µm) supernatants obtained after SPE degradation with GOx and the control experiments were extracted twice with the three volumes of ethyl acetate. The ethyl acetate fractions were pulled together and evaporated using speedvac vacuum concentrator (ThermoFisher scientific, Waltham, MA, USA). Residue remained after evaporation was dissolved in the suitable amount of methanol and the organic products were identified and quantified using GC-MS analysis. GC analyses were performed on a 7890A gas chromatograph (Agilent Technologies, Santa Clara, CA, USA) coupled with an HP 5975 mass selective detector. Injections were carried out with a HP 7693A auto-sampler. The capillary column was an Agilent DB-624 UI column (1.40 µm, 30 m × 0.25 mm i.d.). Helium was the carrier gas at a flow rate of 1.0 mL/min. The temperature program was: initial temperature, 60 °C for 2 min; ramp at 10 °C/min to 250 °C and held for 9 min; injection temperature, 250 °C; and transfer line, 250 °C. The sample injection volume was 2 µL, and the split injection mode with a split ratio of 2:1 was used. The ionizing voltage was 70 eV. The source temperature was set at 250 °C and MS quadrupole temperature was set at 150 °C. Solvent delay was set 3 min. The compound identification was confirmed using mass spectra from NIST spectra library, mass spectra of authentic standards, and the resulting mass spectra obtained from our experiments.

### 2.7. Fourier-transform infrared (FT-IR) spectroscopy, scanning electron microscopy (SEM), and energy-dispersive X-ray spectroscopy (EDX) analysis

FT-IR spectroscopy was used to confirm incorporation of oxidative functional groups onto the native PE polymer chains. Similarly, the TiO<sub>2</sub> nanoparticles were analyzed before and after GOx immobilization. The characterization of functional groups of the SPE polymer was determined by using a Bruker Hyperion 2000 microscope with a liquid nitrogen cooled MCT detector connected to a Bruker Vertex 70 v FT-IR spectrometer (Billerica, MA, USA). The FT-IR measurements were carried out using a germanium (Ge) ATR (Attenuated Total Reflectance) objective (20x). The view field of the FT-IR microscope was 400 µm × 400 µm. The FT-IR spectra were obtained by signal-averaging 32 scans at a peak resolution of 4 cm<sup>-1</sup> between the wavenumbers of 4000 cm<sup>-1</sup> and 500 cm<sup>-1</sup>. A background scan was performed each time before the sample was scanned, and the final sample spectrum was subtracted from the background scan value. The surface morphology and elemental analysis of SPE powder was analyzed using SEM (S-4700, Hitachi, Japan) coupled with EDX (EX-220 Horiba, Japan). Both native PE and SPE powder samples were analyzed to obtain their chemical composition with respect to C, O, Fe, and S atoms using EDX analyses.



### 3. Results and discussion

#### 3.1. Synthesis of SPE

Native PE powder was activated using a strong sulfonating agent, chlorosulfuric acid, followed by grafting of  $\text{Fe}^{3+}$  onto the polymer chains. Sulfonation of PE involves electrophilic substitution reactions which results into introduction of sulfonic acids, C=C double bonds, and sultones into the polymer backbone (Kaneko et al., 2004). The white colored native PE powder was converted to black colored powder of SPE which was insoluble in water and all common organic solvents (Fig. 1 a). Sulfonation and incorporation of C=C double bonds onto the PE polymer chains was confirmed by FT-IR. The spectra shows three unique sets of peaks at  $1034$  and  $1164\text{ cm}^{-1}$ ,  $1630\text{ cm}^{-1}$ , and  $3367\text{ cm}^{-1}$  which indicate efficient sulfonation and incorporation of double bond and hydroxyl functional groups to the PE, respectively (Fig. 1 b). The sulfonation of PE with fuming sulfuric acid or gaseous  $\text{SO}_3$  resulted in the formation of C=C bonds as reported by Kaneko et al. Fig. 2 shows a SEM images and EDX analyses of the PE and SPE powders. The surface morphology of SPE was appeared to be rough and disintegrated while

NPE remained smooth and intact (Fig. 2 a). The elemental composition of the powder was determined by EDX analyses, considering weight % of C, O, S, and Fe atoms (Fig. 2 b). The S/Fe molar ratio of SPE was in the range of 1.5–2, suggesting grafting of  $\sim 2\text{ Fe}^{3+}$  ions for every sulfonate group introduced in the polymer. In addition, C/S ratio of 6.6 for SPE indicates sulfonation of every third ethylene unit from the polymer. Taken together, the FT-IR and SEM-EDX analyses confirms chlorosulfuric acid dependent oxidation of PE to SPE with incorporation of  $\text{Fe}^{3+}$  as observed in the previous study (Chow et al., 2016, 2018).

#### 3.2. Bio-Fenton degradation of SPE using GOx enzyme

Application of the GOx Bio-Fenton reaction changed the black color of SPE powder to brown, indicating degradation of SPE, while the no GOx treated SPE remains black colored (Fig. 3 a). The amount of  $\text{H}_2\text{O}_2$  produced in-situ during the GOx Bio-Fenton reaction was measured using Amplex® red hydrogen peroxide/peroxidase assay kit. In absence of SPE and external ferric citrate, about  $8\text{ mM}$  of  $\text{H}_2\text{O}_2$  was produced from  $32\text{ mM}$  of glucose with  $10\text{ U}$  of GOx under standard assay conditions (Fig. 3a). The pH of the reaction mixture was dropped gradually over the

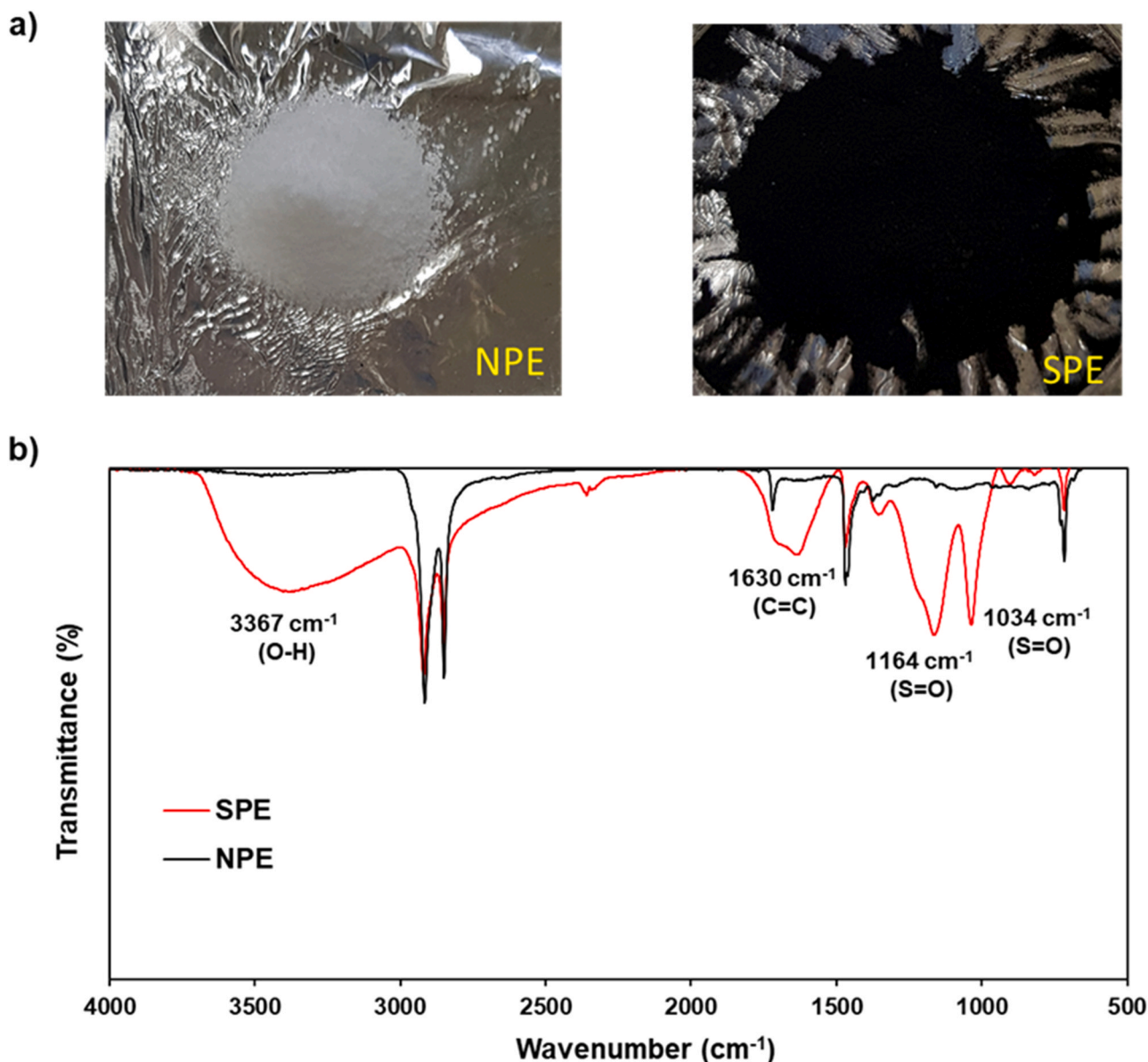


Fig. 1. (a) Picture images showing native PE (NPE) and sulfonated and iron grafted PE (SPE) powder, and (b) FT-IR spectra of NPE and SPE powder.

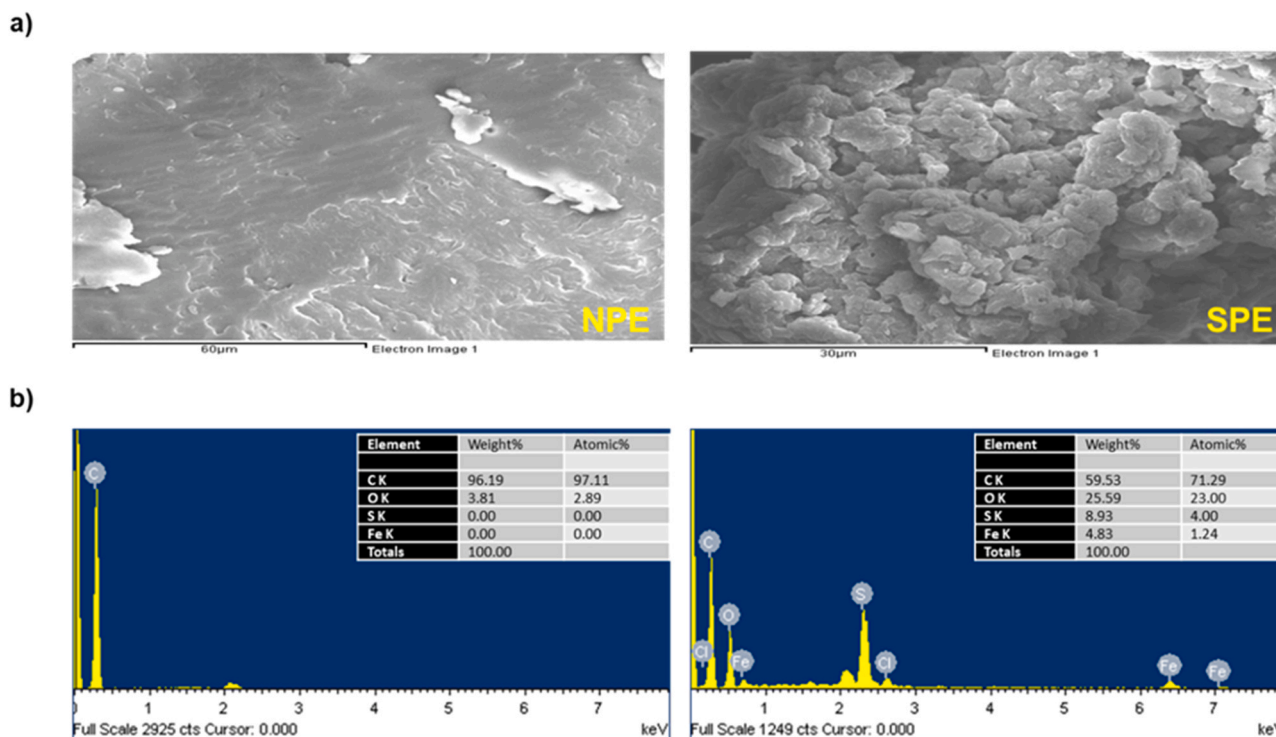


Fig. 2. (a) SEM images showing native PE (NPE) and sulfonated and iron grafted PE (SPE) powder, and (b) EDX analyses of NPE (bottom left) and SPE (bottom right) powder with respect to weight % of C, O, S, and Fe atoms.

period of time and reached to 3.0–3.2 at the end of the assay, mainly due to the formation of gluconate (Fig. 3b). Indeed, the decrease of pH during GOx Bio-Fenton reaction is advantageous as the optimal catalytic activity of Fenton process was observed at pH 3. This is mainly due to the presence of higher concentrations of ferrous and ferric ions in acidic solution, compared other pH values. In addition, the oxidation potential and the oxidation capacity of  $\bullet\text{OH}$  radicals increases with decreasing pH (Pignatelli et al., 2006; Duysterberg et al., 2008). GC-MS analyses indicated that the majority of the hydrolysate of SPE was composed of organic carboxylic acids, particularly monocarboxylic acids such as acetic acid and butanoic acid (Fig. 4, Chromatogram a). The metabolites were identified using MS fragmentation patterns of the extract obtained from SPE degradation after GOx Bio-Fenton incubation for 48 h (Fig. S1), as compared with standard authentic chemicals and NIST library. In addition, the results confirm the formation of the products with carbon atoms ranging from C2–C16. Acetic acid and butanoic acid in the final concentrations at 6.02 mM and 0.19 mM, respectively, were released from SPE. Compounds like isovaleric acid, and 1, 2-ethanediol, monoacetate were present only in a detectable amount below the limit of quantification, and defined as detectable metabolites. In addition, dodecanal and dodecanoic acid was also detected, which could be originated from the radical driven repolymerization of the small organic acids released during the degradation of SPE. Notably, a commonly used plasticizer, dibutyl phthalate was also found in the degraded extract (Table 1). The control experiments with glucose, ferric-citrate, GOx, and no SPE show negligible amounts of acetic acid which might be produced from non-specific attacks of hydroxyl radicals on the reaction components (Fig. 4 Chromatogram b). Notably, GOx alone treatments without SPE did not produce metabolites formed in the GOx Bio-Fenton incubation with SPE (Fig. 4 Chromatogram c). The chromatogram also shows absence of any oligomeric forms of SPE, which was reported previously (Chow et al., 2016, 2018). Taken together, the results evidently suggest that the majority of metabolites obtained herein are acetic acid and butanoic acids released from SPE by GOx Bio-Fenton degradation.

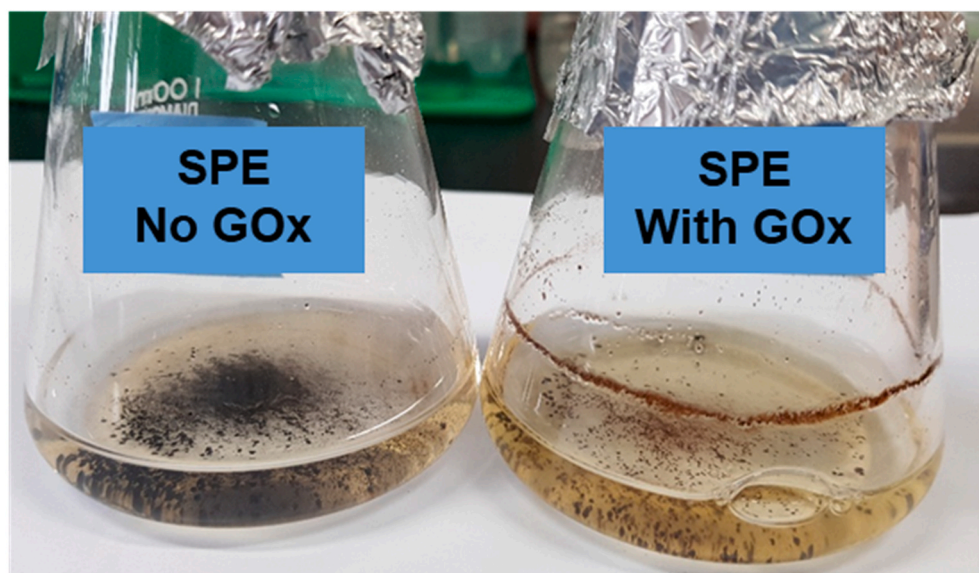
The formation of acetic acid and butanoic acid was increased

proportionally with time (Table 1). With increase in amounts of GOx, the amounts of acetic acid and butanoic acid released from SPE were increased proportionally along with in-situ  $\text{H}_2\text{O}_2$  production. About 2.03 mM of acetic acid and 0.01 mM of butanoic acid were released from 10 mg of SPE using 2.5 U of GOx. With 10 U of GOx, the production of acetic acid and butanoic acid was increased over 3 fold (6.02 mM) and 30 fold (0.19 mM), respectively (Fig. S2). Hence, based on the amount of metabolites formed from SPE, the amount of GOx enzyme, the incubation time, and the amount of in-situ production of  $\text{H}_2\text{O}_2$  are stoichiometrically correlated each other, leading to Bio-Fenton degradation of SPE. It should be noted that the enzyme was precipitated with SPE during the time course experiments, thus limiting the measurement of the amount of SPE remained.

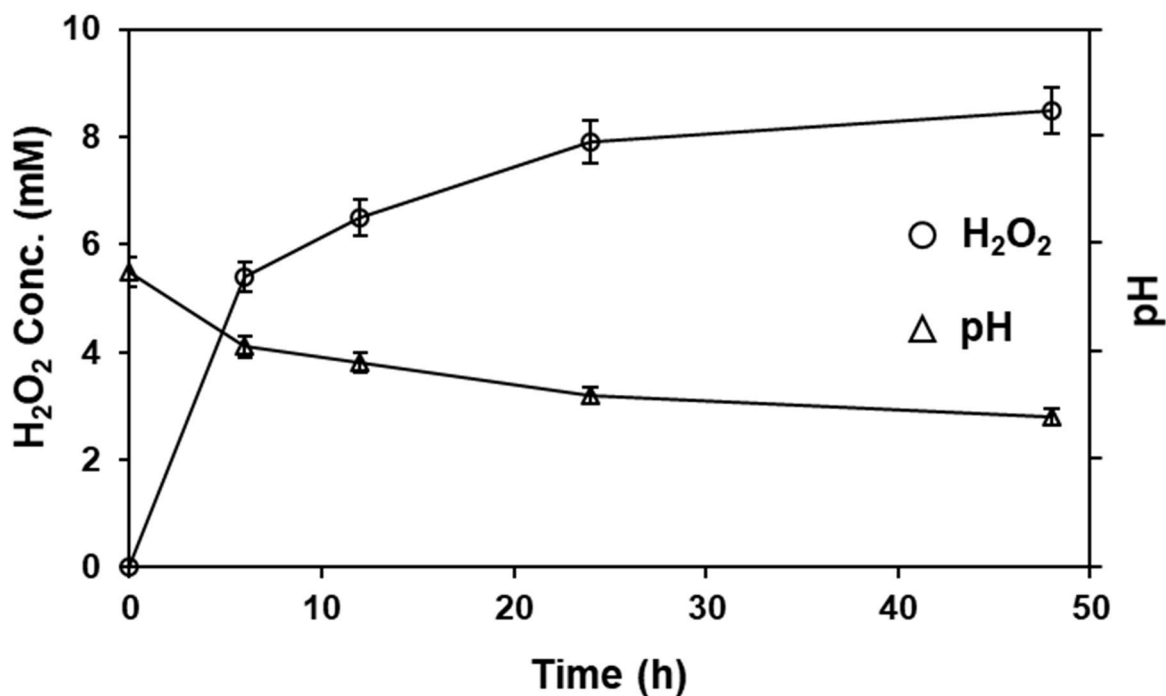
### 3.3. Bio-Photo-Fenton degradation of SPE using $\text{TiO}_2$ -GOx

Fenton and UV assisted Photo-Fenton processes were demonstrated to be capable of efficiently mineralizing various  $\text{Fe}^{3+}$  grafted sulfonated plastic materials such as PS, PP, PVC and PE into fine chemicals and  $\text{CO}_2$  (Feng et al., 2011; Chow et al., 2016, 2018). However, there was no report on using enzymatic Bio-Photo-Fenton degradation approach for degrading PE plastics.  $\text{TiO}_2$  nanoparticles is of a great interest in photocatalytic advanced oxidation processes (AOPs) due to its high efficiency, photocatalytic ability, and high stability in the harsh chemical environments (Gupta and Tripathi, 2011). The low cost, non-toxicity, biocompatibility, and good stability compared to other photo-catalysts,  $\text{TiO}_2$  nanomaterials are widely used as a supporting carrier for enzyme immobilization, including GOx (Gupta and Tripathi, 2011; Abdullah and Kamarudin, 2017). Herein, we investigated Bio-Photo-Fenton degradation of SPE using  $\text{TiO}_2$ -GOx under UV radiation. FT-IR spectra with peaks at  $1650\text{ cm}^{-1}$  and  $1530\text{ cm}^{-1}$  for the  $\text{TiO}_2$ -GOx provide a strong evidence for the successful immobilization of GOx on the surface of the  $\text{TiO}_2$  nanoparticles (Fig. S3) (Kong and Yu, 2007; Baker et al., 2014). The Bio-Photo-Fenton degradation of SPE was studied for different incubation times of 2, 4, and 6 h under UV radiation

a)



b)

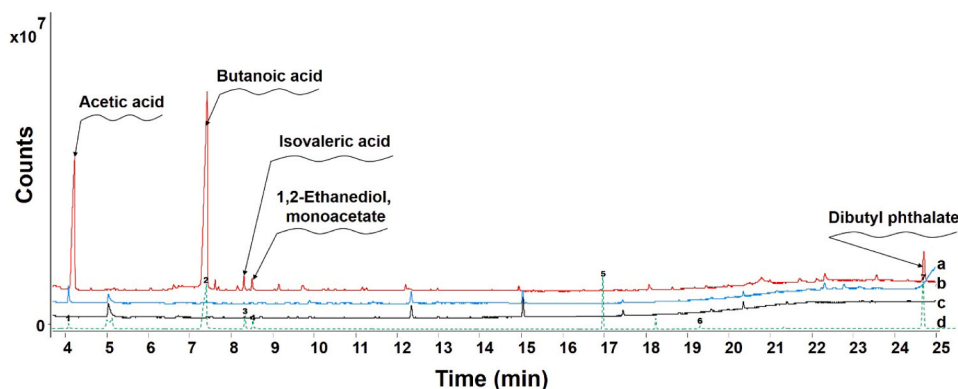


**Fig. 3.** (a) Color change of SPE after Bio-Fenton degradation using free GOx for 48 h. (b) In-situ H<sub>2</sub>O<sub>2</sub> production (circles) and change of pH (triangles) during the Bio-Photo-Fenton degradation using free GOx in the presence of SPE at different incubation time.

with 10 U of TiO<sub>2</sub>-GOx. GC-MS analyses for the Bio-Photo-Fenton degradation of SPE shows significantly higher amounts of acetic acid and butanoic acid (Fig. 5 Chromatogram a), compared to the Bio-Fenton reaction system with free GOx and only TiO<sub>2</sub> nanoparticle control experiment (Fig. 5 Chromatogram b and c). After 6 h of the Bio-Photo-Fenton reaction, 4.78 mM and 0.17 mM of acetic acid and butanoic acid were released, respectively (Table 2). Compared to the Bio-Fenton degradation using free GOx, about 21 fold and 17 fold higher amount of acetic acid and butanoic acid was released by the Bio-Photo-Fenton reaction at 6 h incubation. These results indicate that UV radiation and TiO<sub>2</sub>-GOx synergistically cooperate for the enhanced production of ROS (Kim et al., 2019), resulting in significantly increased

production of small chemicals from SPE. It has been known that direct UV radiation helps convert H<sub>2</sub>O<sub>2</sub> to •OH radicals (Zuo and Hoigné, 1992). In addition, the effect of UV radiation on degradation of SPE by free GOx was also investigated. The amounts of acetic acid (0.31 mM) and butanoic acid (0.01 mM) were much lower than those released from the Bio-Photo-Fenton reaction, but were equal to those of free GOx without UV radiation, after 6 h incubation (Fig. S4a and Table 1). This suggests the poor performance of free GOx under UV radiation to produce H<sub>2</sub>O<sub>2</sub>, probably due to instability of GOx enzyme by UV exposure. It is well known that the enzyme immobilization not only confers to hold the enzyme on the carrier surface by adsorption or/and covalent bonding, but also improve its stability (Cantone et al., 2013). Thus,



**Table 1**

Amount of metabolites released from SPE using Bio-Fenton degradation system using free GOx with different incubation times.

Name of compound	Number of carbons	Retention time (min)	Products (mM) released from SPE using free GOx with different incubation time at			
			6 h	12 h	24 h	48 h
Acetic acid	C2	4.05	0.22	1.92	1.75	6.02
Butanoic acid	C4	7.43	0.01	0.05	0.04	0.19
Isovaleric acid	C5	8.31	–	d	d	d
1,2-Ethanedio, monoacetate	C4	8.51	–	d	d	d
Dodecanal	C12	16.75	d	–	0.01	–
Dodecanoic acid	C12	19.05	–	–	d	–
Dibutyl phthalate	C16	24.71	–	–	–	0.01

– Represent metabolite is not present; d represents metabolite present in detectable amount below the limit of quantification.

immobilization of GOx on TiO<sub>2</sub> nanoparticles makes it a more stable catalyst compared to free GOx, under UV radiation (Fig S4b). Based on the identification and quantification of the metabolites released from SPE after Bio-Fenton degradation using GOx enzyme, we proposed a possible degradation pathway for SPE degradation (Fig. 6). The C/S ratio of 6.6 of SPE suggests incorporation of one SO<sub>3</sub> group into PE after every 6 or 7 carbon atoms in the polymer chain. It is possible that the spacing between two SO<sub>3</sub> groups may vary between 6 and 8 as discussed previously (Chow et al., 2016, 2018). Degradation of SPE possibly occurred via the alpha-, beta-, or gamma- scission of C=C double bonds adjacent to Fe (III) sulfonate groups in the polymer backbone leading to the production of various mono-carboxylic acids such as acetic acid and butanoic acids. Considering •H-abstraction and •OH α-scission reactions, butanoic acid could be formed through cleavage at α-C on the

SPE (Arnold et al., 1995; Chow et al., 2016). Once butanoic acid is formed, it can be converted to either isovaleric acid or 1,2-ethanedio, monoacetate, which can be further filtered into acetic acid through series of alkylation/dealkylation and dehydroxylation/hydroxylation reactions. In addition, acetic acid can be formed directly from butanoic acid with the possible β-scission reaction via dealkylation (Arnold et al., 1995). The hydroxycarboxylic-Fe-sulfonates released during Bio-Fenton and Bio-Photo-Fenton degradation of SPE can be converted to small carboxylic acids such as formic acid and oxalic acid, or even completely mineralized to CO<sub>2</sub> by non-specific attack of •OH radicals as described previously (Chow et al., 2016).

Until now, chemical catalysis coupled with pyrolysis have been extensively studied for degradation of PE to high value liquid fuels and fine chemicals (Jia et al., 2016, 2021). These catalytic pyrolysis processes involve use of elevated temperatures (>300 °C) (Marcilla et al.,

**Table 2**

Amount of metabolites released from SPE using Bio-Photo-Fenton degradation system using TiO<sub>2</sub>-GOx with different UV exposure times.

Name of compound	Products (mM) released from SPE using TiO <sub>2</sub> -GOx with different UV exposure time at		
	2 h	4 h	6 h
Acetic acid	0.38	3.56	4.78
1-Butanol	–	–	d
Butanoic acid	d	0.14	0.17
Isovaleric acid	–	d	0.07
1,2-Ethanedio, monoacetate	–	d	d
Dodecanal	–	d	d
Dibutyl phthalate	–	–	d

– Represent metabolite is not present; d represents metabolite present in detectable amount below the limit of quantification.

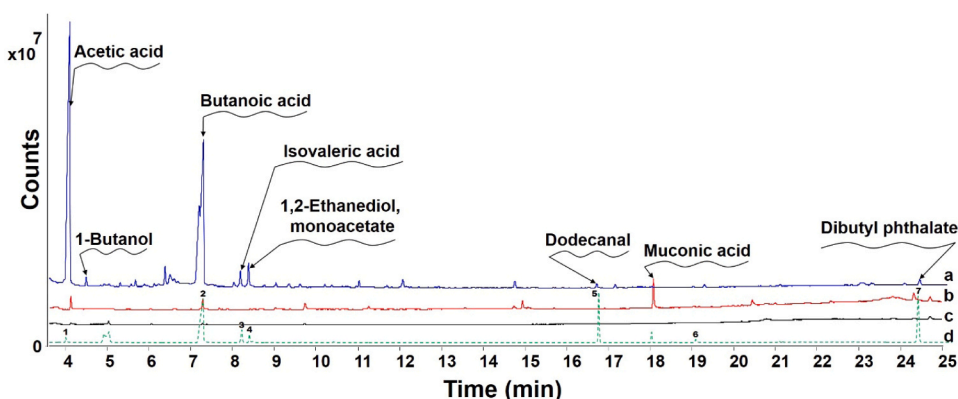


**Fig. 5.** GC chromatogram of metabolites released from Bio-Photo-Fenton degradation containing (a) TiO<sub>2</sub>-GOx in the presence of SPE, (b) the control experiments containing free GOx in the presence of SPE, (c) the control experiments containing TiO<sub>2</sub> nanoparticles alone in the presence of SPE, for 6 h incubation. Arrows indicates peaks corresponding to the respective metabolites, and (d) mixture of standard authentic compounds as (1) acetic acid, (2) butanoic acid, (3) isovaleric acid, (4) 1,2-ethanedio, monoacetate, (5) dodecanal, (6) dodecanoic acid, and (7) dibutyl phthalate.

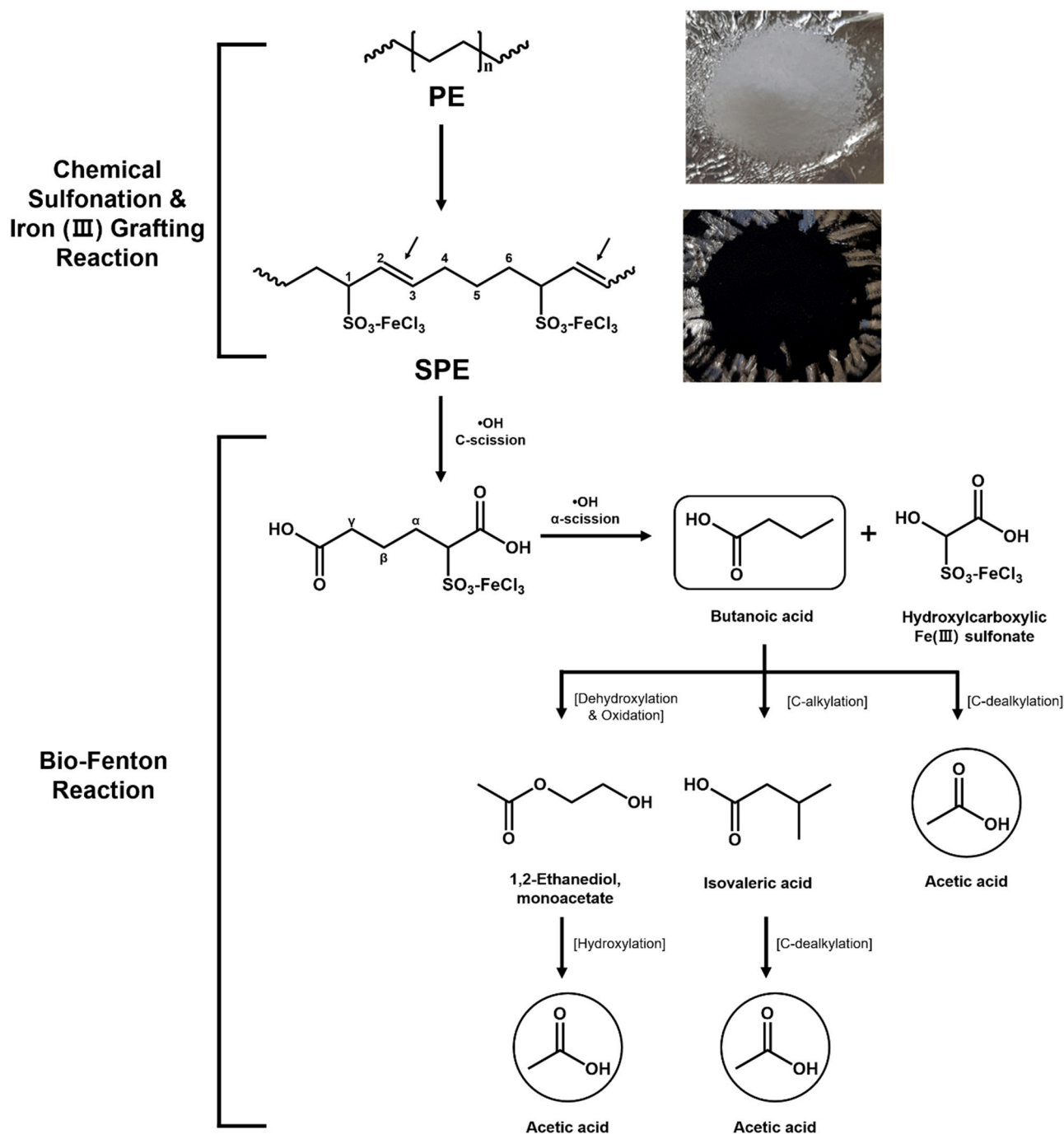


**Fig. 6.** Proposed pathways for SPE degradation using Bio-Photo-Fenton reactions leading to the formation of acetic acid and butanoic acid. The arrows on the chemical structures indicates possible C-C bond cleavage sites for the Fenton reactions.

2009; Zhang et al., 2019), which are not economical. Also it is difficult to control product distribution at high temperatures, resulting into formation of branched, cyclic, and aromatic hydrocarbons (Kaminsky and Zorriquetta, 2007; Park et al., 2019), which can cause catalyst deactivation (Castaño et al., 2011; Ibáñez et al., 2014). In contrast, the current enzymatic Bio-Photo-Fenton degradation approach carried out at ambient temperature of 30 °C released limited metabolites mainly composed of the monocarboxylic acids such as acetic acid and butanoic acids from SPE degradation. However, the conversion efficiency, loss of GOx enzyme, energy input in term of UV, and consumption of glucose can be considered as a limitation in terms of large scale production of small organic acid from sulfonated PE. However, the current approach could pave the way for Bio-Photo-Fenton assisted degradation of

naturally weathered oxidized polyethylene wastes.

Considering biodegradation of chemically inert PE plastics, the plastics should enter cytoplasm of microbial cells to participate into the cellular metabolism or is (bio)chemically modified into smaller molecules outside cells. Direct participation of the PE plastics into cellular metabolism occurred inside cells could be impossible because of insoluble and gigantic size of the PE plastics. Therefore, it is reasonable to assume that modification of the PE plastics should be first occurred outside microbial cells with excreted oxygenase enzymes under aerobic conditions for the PE plastics to participate into cellular metabolism. It has been well known that microbial systems with heme-dependent oxygenase proteins or non-heme oxygenase proteins, which are mostly involved in the initiation of diverse pollutants including



polyaromatic hydrocarbons, long chain alkanes, etc, with incorporation of oxygen into the molecules, requires cofactors for example NADH, etc. It is reasonable to assume that the microbial system has not been evolved into the system expensing the vital resource, cofactor NADH, outside microbial cells. Thus, microbial (biochemical) production and excretion of  $\text{H}_2\text{O}_2$ , followed by the formation of  $\bullet\text{OH}$  radicals through the Fenton reaction could be a rational approach to initiate (bio)degradation of PE plastics with oxygenation under aerobic conditions. Indeed, there are diverse microorganisms with different types of oxygenase enzymes that can produce  $\text{H}_2\text{O}_2$ .

Taken together, microbial cells that excrete  $\text{H}_2\text{O}_2$  into environmental medium under aerobic conditions could be an indispensable natural resource to (bio)degrade naturally weathered and oxidized polyethylene plastic wastes once  $\text{H}_2\text{O}_2$  converts to  $\bullet\text{OH}$  radicals through both photochemistry and Fenton chemistry reactions.

#### 4. Conclusion

We applied Bio-Fenton reactions using free GOx and Bio-Photo-Fenton reactions using  $\text{TiO}_2$ -GOx with exposure of UV light to degrade pre-oxidized PE with sulfonation (SPE) into small carboxylic acids. GC-MS analyses identified acetic acid and butanoic acid as a major products released from the SPE. Comparing the two methods, Bio-Photo-Fenton reactions using  $\text{TiO}_2$ -GOx with exposure of UV light shows the faster degradation of SPE into 4.78 mM of acetic acid and 0.17 mM of butanoic acid after 6 h of incubation. Therefore, the current study could shed lights on (bio)degradation of naturally weathered and oxidized polyethylene plastic wastes to small chemicals using combined reactions with biochemistry, photochemistry, and Fenton chemistry.

#### CRediT authorship contribution statement

HGH proposed and guided the research and revised the manuscript. SSG performed most of the experiments and drafted the manuscript. HGH, SSG, Youri Yang, YK took parts in interpretation and drawing proposed degradation mechanism of SPE. Youri Yang and SSG prepared graphical abstract for the manuscript. YY, JHA, and JJK revised the manuscript. All authors checked the manuscript.

#### Declaration of Competing Interest

The authors declare that they have no known competing financial interests or personal relationships that could have appeared to influence the work reported in this paper.

#### Acknowledgements

This study was carried out with the support (PJ01497402 and PJ0162642021) of National Institute of Agricultural Sciences, Rural Development Administration, Republic of Korea.

#### Appendix A. Supporting information

Supplementary data associated with this article can be found in the online version at [doi:10.1016/j.jhazmat.2021.127067](https://doi.org/10.1016/j.jhazmat.2021.127067).

#### References

Abdullah, M., Kamarudin, S.K., 2017. Titanium dioxide nanotubes (TNT) in energy and environmental applications: an overview. *Renew. Sust. Energ. Rev.* 76, 212–225.  
 Aguado, J., Serrano, D.P., Escola, J.M., 2008. Fuels from waste plastics by thermal and catalytic processes: a review. *Ind. Eng. Chem. Res.* 47, 7982–7992.  
 Albertsson, A.C., Andersson, S.O., Karlsson, S., 1987. The mechanism of biodegradation of polyethylene. *Polym. Degrad. Stab.* 18, 73–87.  
 Albertsson, A.C., Karlsson, S., 1990. The influence of biotic and abiotic environments on the degradation of polyethylene. *Prog. Polym. Sci.* 15, 177–192.

Arnold, S.M., Hickey, W.J., Harris, R.F., 1995. Degradation of atrazine by Fenton's reagent: condition optimization and product quantification. *Environ. Sci. Technol.* 29, 2083–2089.  
 Babuponnusami, A., Muthukumar, K., 2014. A review on Fenton and improvements to the Fenton process for wastewater treatment. *J. Environ. Chem. Eng.* 2, 557–572.  
 Baker, M.J., Trevisan, J., Bassan, P., Bhargava, R., Butler, H.J., Dorling, K.M., Fielden, P. R., Fogarty, S.W., Fullwood, N.J., Heys, K.A., Hughes, C., Lasch, P., Hirsch, P.L.M., Obinaju, B., Sockalingum, G.D., Suso, J.S., Strong, R.J., Walsh, M.J., Wood, B.R., Gardner, P., Martin, F.L., 2014. Using Fourier transform IR spectroscopy to analyze biological materials. *Nat. Protoc.* 9, 1771–1791.  
 Bankar, S.B., Bule, M.V., Singhal, R.S., Ananthanarayan, L., 2009. Glucose oxidase - an overview. *Biotechnol. Adv.* 27, 489–501.  
 Baranowski, A., Klein, A., Ritz, U., Ackermann, A., Anthonissen, J., Kaufmann, K.B., Brendel, C., Götz, H., Rommens, P.M., Hofmann, A., 2016. Surface functionalization of orthopedic titanium implants with bone sialoprotein. *PLoS One* 11, 0153978.  
 Brown, B.S., Mills, J., Hulse, J.M., 1974. Chemical and biological degradation of waste plastics. *Nature* 250, 161–163.  
 Burek, B.O., Bormann, S., Hollmann, F., Bloh, J.Z., Holtmann, D., 2019. Hydrogen peroxide driven biocatalysis. *Green. Chem.* 21, 3232–3249.  
 Cantone, S., Ferrario, V., Corici, L., Ebert, C., Fattor, D., Spizzzo, P., Gardossi, L., 2013. Efficient immobilization of industrial biocatalysts: criteria and constraints for the selection of organic polymeric carriers and immobilization methods. *Chem. Soc. Rev.* 42, 6262–6276.  
 Castaño, P., Elordi, G., Olazar, M., Aguayo, A.T., Pawelec, B., Bilbao, J., 2011. Insights into the coke deposited on HZSM-5, H $\beta$  and HY zeolites during the cracking of polyethylene. *Appl. Catal. B Environ.* 104, 91–100.  
 Chan, J.C., Paice, M., Zhang, X., 2020. Enzymatic oxidation of lignin: challenges and barriers toward practical applications. *Chem. Cat. Chem.* 12, 401–425.  
 Chow, C.F., Wong, W.L., Chan, C.W., Chan, C.S., 2018. Converting inert plastic waste into energetic materials: a study on the light-accelerated decomposition of plastic waste with the Fenton reaction. *Waste Manag.* 75, 174–180.  
 Chow, C.F., Wong, W.L., Ho, K.Y.F., Chan, C.S., Gong, C.B., 2016. Combined chemical activation and Fenton degradation to convert waste polyethylene into high-value fine chemicals. *Chem. Eur. J.* 22, 9513–9518.  
 Condon, S., 1987. Responses of lactic acid bacteria to oxygen. *FEMS Microbiol. Rev.* 46, 269–280.  
 Danso, D., Chow, J., Streit, W.R., 2019. Plastics: environmental and biotechnological perspectives on microbial degradation. *Appl. Environ. Microbiol.* 85, 1–14.  
 Deng, Y., Englehardt, J.D., 2006. Treatment of landfill leachate by the Fenton process. *Water Res.* 40, 3683–3694.  
 Dong, C., Xing, M., Zhang, J., 2020. Recent progress of photocatalytic Fenton-like process for environmental remediation. *Front. Environ. Chem.* 1, 8.  
 Duesterberg, C.K., Mylon, S.E., Waite, T.D., 2008. pH Effects on iron-catalyzed oxidation using Fenton's reagent. *Environ. Sci. Technol.* 42, 8522–8527.  
 Eskandarian, M., Mahdizadeh, F., Ghalamchi, L., Naghavi, S., 2013. Bio-Fenton process for Acid Blue 113 textile azo dye decolorization: characteristics and neural network modeling. *Desalin. Water Treat.* 52, 4990–4998.  
 Feng, H.M., Zheng, J.C., Lei, N.Y., Yu, L., Kong, K.H.K., Yu, H.Q., Lau, T.C., Lam, M.H.W., 2011. Photoassisted Fenton degradation of polystyrene. *Environ. Sci. Technol.* 45, 744–750.  
 Geyer, R., Jambeck, J., Law, K.L., 2017. Production, use, and fate of all plastics ever made. *Sci. Adv.* 3, 1–5.  
 Ghatge, S., Yang, Y., Ahn, J.H., Hur, H.G., 2020. Biodegradation of polyethylene: a brief review. *Appl. Biol. Chem.* 63, 1–14.  
 Gu, C., Wang, J., Liu, S., Liu, G., Lu, H., Jin, R., 2016. Biogenic Fenton-like reaction involvement in cometabolic degradation of tetrabromobisphenol A by *Pseudomonas* sp. *Environ. Sci. Technol.* 50, 9981–9989.  
 Gupta, S.M., Tripathi, M., 2011. A review of  $\text{TiO}_2$  nanoparticles. *Chin. Sci. Bull.* 56, 1639–1657.  
 Hertzberger, R., Arents, J., Dekker, H.L., Pridmore, R.D., Gysler, C., Kleerebezem, M., Mattos, M.J.T.D., 2014.  $\text{H}_2\text{O}_2$  production in species of the *Lactobacillus acidophilus* group: a central role for a novel NADH-dependent flavin reductase. *Appl. Environ. Microbiol.* 80, 2229–2239.  
 Hu, Y., Xiang, M., Jin, C., Chen, Y., 2015. Characteristics and heterologous expressions of oxalate degrading enzymes "oxalate oxidases" and their applications on immobilization, oxalate detection, and medical usage potential. *J. Biotech. Res.* 6, 63–75.  
 Huang, J., Wang, H., Li, D., Zhao, W., Ding, L., Han, Y., 2011. A new immobilized glucose oxidase using  $\text{SiO}_2$  nanoparticles as carrier. *Mater. Sci. Eng. C* 31, 1374–1378.  
 Ibáñez, M., Artetxe, M., Lopez, G., Elordi, G., Bilbao, J., Olazar, M., Castaño, P., 2014. Identification of the coke deposited on an HZSM-5 zeolite catalyst during the sequenced pyrolysis-cracking of HDPE. *Appl. Catal. B Environ.* 148–149, 436–445.  
 Jambeck, J.R., Geyer, R., Wilcox, C., Siegler, T.R., Perryman, M., Andrady, A., Narayan, R., Law, K.L., 2015. Marine pollution. Plastic waste inputs from land into the ocean. *Science* 347, 768–771.  
 Jaquish, R., Reilly, A.K., Lawson, B.P., Golikova, E., Sulman, A.M., Stein, B.D., Lakina, N. V., Tkachenko, O.P., Sulman, E.M., Matveeva, V.G., Bronstein, L.M., 2018. Immobilized glucose oxidase on magnetic silica and alumina: beyond magnetic separation. *Int. J. Biol. Macromol.* 120, 896–905.  
 Jeon, H.J., Kim, M.N., 2015. Functional analysis of alkane hydroxylase system derived from *Pseudomonas aeruginosa* E7 for low molecular weight polyethylene biodegradation. *Int. Biodeterior. Biodegrad.* 103, 141–146.  
 Jia, C., Xie, S., Zhang, W., Intan, N.N., Sampath, J., Pfandtnr, J., Lin, H., 2021. Deconstruction of high-density polyethylene into liquid hydrocarbon fuels and lubricants by hydrogenolysis over Ru catalyst. *Chem. Catal.* 1, 241–257.

- Jia, X., Qin, C., Friedberger, T., Guan, Z., Huang, Z., 2016. Efficient and selective degradation of polyethylenes into liquid fuels and waxes under mild conditions. *Sci. Adv.* 2, 1501591.
- Kahousha, M., Beharya, N., Caylaa, A., Nierstrasz, V., 2018. Bio-Fenton and Bio-electro-Fenton as sustainable methods for degrading organic pollutants in wastewater. *Process Biochem* 64, 237–247.
- Kaminsky, W., Zorriquetta, I.J.N., 2007. Catalytical and thermal pyrolysis of polyolefins. *J. Anal. Appl. Pyrolysis* 79, 368–374.
- Kaneko, M., Kumagai, S., Nakamura, T., Sato, H., 2004. Study of sulfonation mechanism of low-density polyethylene films with fuming sulfuric acid. *J. Appl. Poly. Sci.* 91, 2435–2442.
- Karimi, A., Aghbolaghy, M., Khataee, A., Bargh, S.S., 2012. Use of enzymatic bio-Fenton as a new approach in decolorization of malachite green. *Sci. World J.* 2012, 1–5.
- Kavitha, V., Palanivelu, K., 2004. The role of ferrous ion in Fenton and photo-Fenton processes for the degradation of phenol. *Chemosphere* 55, 1235–1243.
- Kim, B.C., Jeong, E., Kim, E., Hong, S.W., 2019. Bio-organic-inorganic hybrid photocatalyst, TiO<sub>2</sub> and glucose oxidase composite for enhancing antibacterial performance in aqueous environments. *Appl. Catal. B Environ.* 242, 194–201.
- Kong, J., Yu, S., 2007. Fourier transform infrared spectroscopic analysis of protein secondary structures. *Acta Biochim. Biophys. Sin.* 39, 549–559.
- Krueger, M.C., Harms, H., Schlosser, D., 2015. Prospects for microbiological solutions to environmental pollution with plastics. *Appl. Microbiol. Biotechnol.* 99, 8857–8874.
- Lee, B., Pometto, A.L., Fratzke, A., Bailey, T.B., 1991. Biodegradation of degradable plastic polyethylene by *Phanerochaete* and *Streptomyces* species. *Appl. Environ. Microbiol.* 57, 678–685.
- Lönnstedt, O.M., Eklöv, P., 2016. Environmentally relevant concentrations of microplastic particles influence larval fish ecology. *Science* 352, 1213–1216.
- Marcilla, A., Beltrán, M.I., Navarro, R., 2009. Thermal and catalytic pyrolysis of polyethylene over HZSM5 and HUSY zeolites in a batch reactor under dynamic conditions. *Appl. Catal. B Environ.* 86, 78–86.
- Mehmet, D., 2011. 100+ Years of Plastics: Leo Baekeland and Beyond, 1080. American Chemical Society, Washington, DC, pp. 115–145.
- Nidheesh, P.V., 2015. Heterogeneous Fenton catalysts for the abatement of organic pollutants from aqueous solution: a review. *RSC Adv.* 5, 40552–40577.
- North, E.J., Halden, R.U., 2013. Plastics and environmental health: the road ahead. *Rev. Environ. Health* 28, 1–8.
- Park, K.B., Jeong, Y.S., Guzelciftci, B., Kim, J.S., 2019. Characteristics of a new type continuous two-stage pyrolysis of waste polyethylene. *Energy* 166, 343–351.
- Pignatelli, J.J., Oliveros, E., Mackay, A., 2006. Advanced oxidation processes for organic contaminant destruction based on Fenton reaction and related chemistry. *Crit. Rev. Environ. Sci. Technol.* 36, 1–84.
- Rahimi, A., García, J.M., 2017. Chemical recycling of waste plastics for new materials production. *Nat. Rev. Chem.* 1, 0046.
- Ravi, S., Lonappan, L., Touahar, L., Fonteneau, E., Vaidyanathan, V.K., Cabana, H., 2020. Evaluation of bio-fenton oxidation approach for the remediation of trichloroethylene from aqueous solutions. *J. Environ. Manag.* 270, 110899.
- Restrepo-Florez, J.M., Bassi, A., Thompson, M.R., 2014. Microbial degradation and deterioration of polyethylene – a review. *Int. Biodeterior. Biodegrad.* 88, 83–90.
- Santo, M., Weitsman, R., Sivan, A., 2013. The role of the copper-binding enzyme laccase in the biodegradation of polyethylene by the actinomycete *Rhodococcus ruber*. *Int. Biodeterior. Biodegrad.* 84, 204–210.
- Sen, S.K., Raut, S., 2015. Microbial degradation of low density polyethylene (LDPE): a review. *Environ. Chem. Eng.* 3, 462–473.
- Serrano, D.P., Aguado, J., Escola, J.M., 2012. Developing advanced catalysts for the conversion of polyolefinic waste plastics into fuels and chemicals. *ACS Catal.* 2, 1924–1941.
- Su, Q., Klinman, J.P., 1999. Nature of oxygen activation in glucose oxidase from *Aspergillus niger*: the importance of electrostatic stabilization in superoxide formation. *Biochemistry* 38, 8572–8581.
- Tokiwa, Y., Calabia, B., Ugwu, C., Aiba, S., 2009. Biodegradability of plastics. *Int. J. Mol. Sci.* 10, 3722–3742.
- Wang, J., Ma, Q., Zhang, Z., Li, S., Diko, C.S., Dai, C., Zhang, H., Qu, Y., 2020. Bacteria mediated Fenton-like reaction drives the biotransformation of carbon nanomaterials. *Sci. Total Environ.* 746, 141020.
- Weber, C., Pusch, S., Opatz, T., 2017. Polyethylene bio-degradation by caterpillars? *Curr. Biol.* 27, 744–745.
- Yoon, M., Jeon, H., Kim, M., 2012. Biodegradation of polyethylene by a soil bacterium and AlkB cloned recombinant cell. *J. Bioremed. Biodegrad.* 3, 145.
- Zepp, R.G., Faust, B.C., Hoigné, J., 1992. Hydroxyl radical formation in aqueous reactions (pH 3–8) of iron(II) with hydrogen peroxide: the photo-Fenton reaction. *Environ. Sci. Technol.* 26, 313–319.
- Zhang, Y., Duan, D., Lei, H., Villota, E., Ruan, R., 2019. Jet fuel production from waste plastics via catalytic pyrolysis with activated carbons. *Appl. Energy* 251, 113337.
- Zheng, Y., Yanful, E.K., Bassi, A.S., 2005. A review of plastic waste biodegradation. *Crit. Rev. Biotechnol.* 25, 243–250.
- Zuo, Y., Hoigné, J., 1992. Formation of hydrogen peroxide and depletion of oxalic acid in atmospheric water by photolysis of iron(III)-oxalato complexes. *Environ. Sci. Technol.* 26, 1014–1022.